CARBON FILMS FOR ELECTRONIC APPLICATIONS

Marie Millares[1], Philip Schneider[1], Iulian Gherasoiu[2] and Harry Efstathiadis[1]

[1]College of Nanoscale Engineering, State University of New York Polytechnic Institute, Albany, NY

[2]College of Engineering, State University of New York Polytechnic Institute, Utica, NY

MMillaresFrancoise@sunypoly.edu

Producing hydrogen directly from water through the use of solar energy from an efficient photoelectrical (PEC) system is key in cultivating a sustainable and renewable economy. Hydrogen sourced energy can have tremendous impact and application on industry, especially concerning fuel cells. However, limitations, such as cell corrosion, prevent this technology from full implementation. This research focuses on the fabrication of Diamond-Like Carbon (DLC) through Plasma-Enhanced Chemical Vapor Deposition (PECVD), which is used as an anti-corrosion layer. By testing different annealing temperatures, we can observe how the carbon structure is affected. It was found that synthesizing DLC at low temperatures (~100^{o}C) in conjunction with annealing enhances diamond structures on the substrate. This allows for an increased resistance towards corrosion and higher transparency within the film.

Graduate student oral presentation

DISCRIMINATION OF TEA AROMAS WITH NANOPARTICLE-BASED ELECTRONIC NOSE

Tuo Gao[1], Chengwu Zhang[1], Yongchen Wang[2], Jing Zhao[2], Ranjan Srivastava[1], Brian G Willis[1]

[1]Department of Chemical and Biomolecular Engineering, [2]Department of Chemistry, University of Connecticut, Storrs, Connecticut, USA 06269

In this work, we demonstrated a nanoparticle-based electronic nose system that distinguishes 35 flavors of teas, ranging from black teas, green teas, and herbal teas. Four types of gold nanoparticles (AuNPs) with chemically diverse ligands were chosen as sensing elements. The functionalization includes DMAP (4-dimethylaminopyridine), ODA (octadecylamine), 3-MPA (3-mercaptopropionic acid), and 4-ATP (4-aminothiophenol). To assemble the electrodes, nanoparticle solutions were drop-cast on the active sensing region that consists of castellated microstructures with 2-μm gap. The sensor chip was designed with separated active sensing regions so that each AuNP can have 12 working sensors maximum. This allowed diversity as well as redundancy for sensing experiment. Fresh tea powders were added to a glass syringe and the dosing was completed by a syringe pump with controlled delivery speed. Dry nitrogen gas was used for purging. Sensing responses, expressed as $\Delta R/R_0$, were measured simultaneously for all sensors using a switch matrix/multimeter system. Raw data processing and statistical analysis were performed using MATLAB to evaluate the performance of the chemiresistive electronic nose array.

Depending on flavors, sensing elements, and baseline resistance difference, $\Delta R/R_0$ of 1-20% were achieved. The resulting variation enables statistical analysis, such as principal component analysis (PCA), linear discriminant analysis (LDA), support vector machine (SVM), and random forest (RF). With five-fold cross validation, we have achieved 99% accuracy with LDA for all 35 flavors of teas. We also found that multi-particle assembly works better than using single type of particles. For example, by choosing two working sensors from each particle, we obtained 91.4 ± 3.3% accuracy for 13 black and green teas, and 88.6 ± 3.7% for 22 herbal teas. On the other hand, if we chose 8 sensors from each of the four particles, the classification accuracy dropped. This is a significant improvement (> 10%) from single particle assembly. The results showed accurate classification of 35 flavors of teas and provided a promising approach to monitor the quality and grade of tea products. Moreover, by increasing the chemical variation in ligands, it is possible to select the ligand combination that gives the best overall performance.

Graduate student oral presentation

RESISTIVITY SCALING IN MULTI-DOMAIN POLYCRYSTALLINE Ir LAYERS

Atharv Jog* and Daniel Gall

Department of Materials Science and Engineering, Rensselaer Polytechnic Institute, 110 8th St, Troy, NY 12180, USA

*joga@rpi.edu

Ir layers are sputter deposited onto polished MgO(001) and Al_2O_3(0001) substrates and their resistivity ρ is measured *in situ* and *ex situ* at 298 K and in liquid N_2 at 77 K as a function of layer thickness d = 5 – 100 nm in order to quantify the resistivity size effect. The resistivity size effect represents a major challenge for continued down scaling of integrated circuits due to increased signal delay and power consumption caused by increasing electron scattering at the surfaces and grain boundaries as the interconnect line widths approach the electron-phonon scattering mean free path λ. Iridium has a low predicted product $\rho_o \times \lambda = 3.69\times 10^{-16}$ Ωm^2, suggesting that contributions from surface and grain boundary scattering to overall resistivity is small. Thus, Ir has great promise as low-resistivity material for highly scaled interconnect lines.

Deposition of Ir at T_s = 700 °C on MgO(001) substrates results in epitaxial Ir(001) layers but with a poor crystalline quality. Increasing the growth temperature to T_s = 1000 °C improves the crystalline quality but leads to dewetting for films with thickness d < 10 nm. Growth on Al_2O_3 (0001) substrates yields Ir(111) layers with a high crystalline quality but a polycrystalline microstructure with two 111-oriented epitaxial domains, causing electron grain boundary scattering. Lastly, Ir deposited on MgO(001) at T_s = 700 °C and stepwise annealed *in situ* to 1000 °C results in a multi-domain polycrystalline microstructure with an excellent crystalline quality that is facilitated by renucleation of Ir grains at the Ir-MgO interface. Despite the grain boundaries, the resistivity increase with decreasing d for this last series is quite small, with ρ = 6.41, 6.70, and 1.87 μΩ-cm for a 9.9-nm-thick Ir layer measured *in situ* and *ex situ* at 298 K and 77 K, respectively. This room temperature value is just 23% above the bulk resistivity ρ_o = 5.2 μΩ-cm, indicating an electron mean free path λ = 5.2 nm. The measured product $\rho_o \times \lambda = 2.70\times 10^{-16}$ Ωm^2 is 27% below the above-mentioned theoretical prediction and 60%, 63%, and 47% below reported measurements for Cu, Co, and Ru, respectively. This demonstrates a very low resistivity scaling for Ir and suggests that the Ir conductivity outperforms these competing metals for narrow interconnect lines.

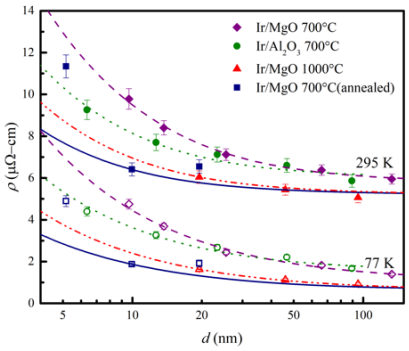

Selectivity Study of Photon-Enhanced Area Selective Atomic Layer Deposition of Plasmonic Nanostructures

Chengwu Zhang, Jie Qi, Tuo Gao and Brian Willis

Chemical & Biomolecular Engineering, University of Connecticut, Storrs, CT, 06269, USA.

Email: chengwu.zhang@uconn.edu

Conventional wafer fabrication involves many process steps. And this top down processing has met challenges to future scaling, such as edge alignment, cost of lithography and step compatibility. Area selective atomic layer deposition (ALD) is one bottom up process to deposit material only where is desired. It can simplify fabrication process and eliminate compatibility issues like use of etchants. Selectivity is essential factor that should be quantified when area selective ALD is used. Current selectivity is compared in terms of film thickness in selective area and non-selective area. However, selectivity in initial nucleation and growth process has not been well studied.

In our study, photon enhanced area selective ALD is used to deposit disc nanostructures. Selective growth on disc nanostructures and non-selective growth on substrate have been defined. When light intensity increases, growth per cycle (GPC) of different sizes of discs increase respectively. And non-selectivity growth becomes significant when light intensity reaches 1.49×10^4 W/m^2. Grain size and density are measured by ProSEM and ImageJ to quantify non-selective growth. At last, selectivity in growth area and non-selective area is compared.

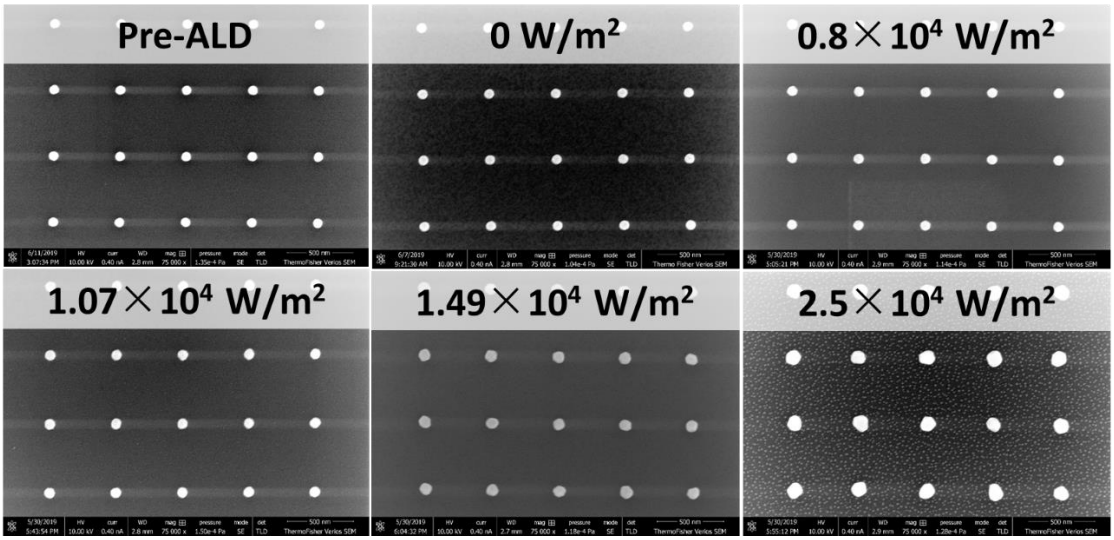

Figure 1. SEM images of area selectivity ALD in different light intensities.

Graduate student oral presentation

Epitaxial growth of cubic WC_y(001) thin films

Peijiao Fang, Daniel Gall

Department of Materials Science and Engineering, Rensselaer Polytechnic Institute

fangp@rpi.edu

Tungsten carbide films were sputter-deposited onto MgO(001) substrates at 400 °C in 5 mTorr Ar-CH_4 gas mixtures with a varying CH_4 fraction f_{CH4} = 0.4 - 6.0 %. High resolution cross-sectional transmission electron microscopy and X-ray diffraction (XRD) ω-2θ scans, ω-rocking curves, and reciprocal space maps (RSM) on 10-nm-thick layers indicate a heteroepitaxial growth of rock-salt WC_y with a cube-on-cube epitaxial relationship: $(001)_{WC}$ || $(001)_{MgO}$ and $[100]_{WC}$ || $[100]_{MgO}$. However, continued growth to a layer thickness d = 600 nm leads to the nucleation of grains with a hexagonal W_2C phase for f_{CH4} < 1 %, and to a nanocrystalline microstructure with cubic WC_y grains embedded in an amorphous carbon a-C:H matrix for f_{CH4} > 1 %. The measured out-of-plane coherence length matches the film thickness for d = 10 nm, and remains nearly unaffected by a 60-fold increase in layer thickness to d = 600 nm, suggesting that the critical thickness for epitaxial breakdown is ~ 10 nm. The relaxed lattice constant of cubic WC_y increases monotonically from 0.419 to 0.425 nm with increasing f_{CH4}. Comparing these measured lattice parameters with predictions from first-principles indicates a C-to-W ratio y = 0.47 - 0.68. However, composition measurements using Energy-dispersive X-ray Spectroscopy, Rutherford Backscattering Spectrometry and Nuclear Reaction Analysis yield measured C-to-W ratios of 0.57-1.25, suggesting that a considerable fraction (18 – 46 %) of C does not incorporate in the cubic phase but may form an amorphous carbon phase.

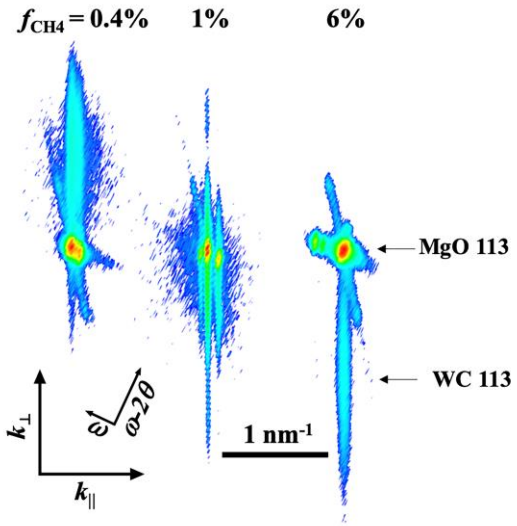

Fig. 1. Representative XRD RSMs of asymmetric 113 reflections from 10-nm-thick WC_y(001)/MgO(001) layers deposited with f_{CH4} = 0.4%, 1%, and 6%.

Graduate student poster

MELT EXTRUSION OF NOVEL THERMAL STIFFENING NANOCOMPOSITES

[1,2]Chen Gong, [3]Pinar Akcora, [1,2]Rahmi Ozisik

[1]Materials Science and Engineering; [2]Center for Materials, Devices, and Integrated Systems; Rensselaer Polytechnic Institute

[3]Chemical Engineering and Materials Science, Stevens Institute of Technology

*email address: gongc2@rpi.edu

A class of polymer-absorbed silica nanoparticle reinforced polymer nanocomposites were found to have a peculiar thermal stiffening response with increasing temperature that not only provides a new method to manipulate mechanical properties as a function of temperature but also offers the opportunity to develop new products based on thermal stiffening. The next step towards mass production requires testing these new class of materials' processability via traditional polymer processing techniques such as extrusion. In the current work, a laboratory mixing extruder was used to evaluate the processability and the effect of processing conditions on thermal stiffening behavior. Polymers with different rigidities were absorbed on to silica nanoparticles before they were dispersed in a poly(ethylene oxide), PEO, matrix. Then these nanocomposites were melt-extruded under various extrusion conditions. The resultant extrudates were characterized using Fourier-transform infrared spectroscopy (FTIR), electron microscopy and small angle x-ray scattering (SAXS). Thermal stiffening behavior of the extrudates were characterized using a parallel plate rheometer. In systems with highly rigid adsorbed polymers, the storage modulus values dropped drastically after extrusion. Whereas systems with less rigid adsorbed polymers recovered and even experienced a slight reinforcement in storage modulus after extrusion. The current work probes the processability of a novel nanocomposite system and also provides new insights into its dynamics under complex deformation conditions.

Graduate student poster

IMPACT OF SURFACE FUNCTIONALITY ON MAGNETIC PROPERTIES OF Fe_3O_4 – POLY(ETHYLENE OXIDE) NANOCOMPOSITES

[1,3]Donovan Weiblen, [2,3]Grace Gionta, [3]Deniz Rende, [4]Pinar Akcora, [2,3]Rahmi Ozisik

[1]Materials Science and Engineering, [2]Chemical Engineering, [3]Center for Materials, Devices and Integrated Systems; Rensselaer Polytechnic Institute, Troy, NY 12180, U.S.A.

[4]Chemical Engineering and Materials Science; Stevens Institute of Technology, Hoboken, NJ 07030, U.S.A.

Presenting author's email: weibld@rpi.edu

There has been increased focus on magnetically activated polymer nanocomposites in recent years. These smart materials exhibit tunable properties and are of interest due to their many possible applications in areas such as shape memory polymers, drug delivery, and membrane technology. The response of magnetic polymer nanocomposites is triggered by external stimuli in the form of an alternating magnetic field. Current work investigates the impact of two surfactants, polyethylene glycol α–, ω–diphosphate, and aminopropyl triethoxysilane on the magnetic heating response of iron oxide (magnetite) nanoparticles dispersed in polyethylene oxide (PEO). These nanoparticles were loaded into PEO at low concentrations varying from 0.010–0.750% by weight. PEO was chosen due to its known biocompatibility and use in the healthcare industry. A significant increase in temperature was observed considering the low loading of particles in all samples. Analysis of heating curves shows that amine functionalization of nanoparticles improves the heat generating efficiency of our magnetic nanocomposites significantly. This unusual behavior of amine coated nanoparticles persists at higher loading concentrations. These results are opposite to the expected decrease of magnetic phase (and therefore heating efficiency) with the addition of surface coatings to magnetite nanoparticles.

Graduate student poster

MAGNETICALLY INDUCED SELF–HEALING OF POLYMERS

[1,3]Charlotte Teunisse, [1,3]Sarah Dalakos, [1,3]Donovan Weiblen, [2,3]Grace Gionta, [3]Deniz Rende, [2,3]Rahmi Ozisik

[1]Materials Science and Engineering, [2]Chemical Engineering, [3]Center for Materials, Devices and Integrated Systems; Rensselaer Polytechnic Institute, Troy, NY 12180, U.S.A.

Presenting author's email: teunic@rpi.edu

Current research aims to quantify self-healing capabilities of iron oxide nanoparticle infused polyethylene oxide. Iron oxide nanoparticles of varying surface chemistries (bare, aminopropyl triethoxysilane coated, and polyethylene glycol α–, ω–diphosphate) are used to prepare nanocomposites of varying concentrations by weight (0.05%, 0.01%, 0.25%, and 0.50%). Each sample is indented with LECO M400 Microindenter at five different locations between the center and edge. The indentation site is examined before and after being placed in an alternate magnetic field (AMF) to induce healing. A control sample of PEO without nanoparticles is also examined before and after exposure to the AMF. The micrographs of each indent were collected with an Olympus PMEG microscope at the same imaging parameters. Healing efficiency is quantified using image analysis with ImageJ. Multiple methods of image analysis have been explored and results were best examined overlaying the before and after images to quantify the percentage of healing as a function nanoparticle concentration.

Undergraduate student poster

COLLOIDAL NANOCRYSTALS

FROM SYNTHESIS TO OPTOELECTRONIC APPLICATIONS

Stefan Kudera

Former Marie-Curie Fellow at the Istituto Italiano di Tecnologia, Genoa, Italy and former group leader at the Max Planck Institut für Intelligente Systeme, Stuttgart, Germany

email: mail@skudera.de

I will present an overview on my work on the dynamics of the synthesis of colloidal nanocrystals in organic solvents, and the ongoing efforts on functionalising surfaces with these nanocrystals.

The synthesis of colloidal nanocrystals offers wide possibilities for the adjustment of the physical and chemical properties of the resulting nanocrystals. I will present two procedures that offer insights in an early stage of the growth, the nucleation. One allows to slow down the growth in order to observe the formation of magic-size-clusters, which can be understood as nanocrystals of particular stability. The second method allows for a controlled introduction of defects during the nucleation, which then result in the formation of branched nanocrystals.[1]

There are two principle pathways for exploiting the properties of the nanocrystals. In the first case, the particles are considered constituents of a larger ensemble and their collective response is used as their signal. An example of this are screens where a certain number of nanocrystals are excited in order to produce a fluorescence signal. The second pathway would be to address individual nanocrystals. For the latter, a higher control over their deposition onto a substrate is required. I will present a method for the deposition of the particles at a controlled density [2] and a method for the analysis of thin, dense films of nanocrystals by scanning photocurrent microscopy [3].

Finally, I will present a method that allows for the post-deposition alteration of the physical properties of nanocrystals, based on cation exchange. The method can be applied to individual nanocrystals [4] or to sections of a film of nanocrystals.

[1] Kudera S, Maus L, Zanella M, Pelaz B, Zhang Q, del Pino P, Parak WJ. Inorganic Core–Shell Nanoparticles. In: Reference Module in Materials Science and Materials Engineering, Elsevier; 2016

[2] Ullrich S, Scheeler SP, Pacholski C, Spatz JP, Kudera S Formation of Large 2D Arrays of Shape-Controlled Colloidal Nanoparticles at Variable Interparticle Distances. Particle & Particle Systems Characterisation. 2013;30: 102–10

[3] Kudera S, Zhang Y, Di Fabrizio E, Manna L, Krahne R Spatial analysis of the photocurrent generation and transport in semiconductor nanocrystal films. Phys. Rev. B. 2012;86: 07

[4] Dogan S, Kudera S, Dang Z, Palazon F, Petralanda U, Artyukhin S, et al. Lateral epitaxial heterojunctions in single nanowires fabricated by masked cation exchange. Nature Communications, 2018;9: 505.

Researcher poster

In situ ToF-SIMS Analysis of FIB Prepared Li Ion Battery Anodes

Vincent S. Smentkowski, Richard Hart, Hongbo Cao

GE – Research, 1 Research Circle, Niskayuna NY 12309

Felix Kollmer, Julia Zakel, Henrik Arlinghaus

IONTOF GmbH, Heisenbergstraße 15, 48149 Münster Germany

Depth profiling (1D or 3D) is often used to determine the depth distribution of species in a material. Depth profiling works well when the surface of a sample is smooth and when the depth(s) are in the nm to micron thickness range. For thicker layers, one can mount the material in epoxy and generate a cross section which can be imaged. Unfortunately, cutting and polishing often damages (or at least smears) fragile materials such Li ion batteries. Over the two past decades, Focused Ion Beam (FIB) has proven to be a viable approach to expose sub surface layers 10s of microns thick which is often analyzed by SEM or TEM in conjunction with EDS [1]. Unfortunately, most EDS detectors are not able to detect light species such as Li and C (especially at the degraded vacuum which most SEM's operate under), and definitely cannot detect H. ToF-SIMS not only detects all elements (and their isotopes), it also allows for the analysis of molecular fragments which is often critical for understanding the material. FIB/ToF-SIMS has been used to analyze other material systems [2, 3].

In this late breaking poster, we will provide preliminary in-situ FIB/ToF-SIMS results which were generated on an anode taken from a Li ion battery. In order to simultaneously obtain high lateral resolution images at high mass resolution, the delayed extraction data collection mode was utilized [4]. The advantages of multivariate statistical analysis (MVSA) for these complex data sets will be demonstrated.

[1] Lucille A. Giannuzzi, and Fred A. Stevie, Eds., "Introduction to Focused Ion Beams", Springer-Verlag US (2005) DOI: https://doi.org/10.1007/b101190.
[2] Felix Kollmer, D. Rading, R. Moellers, H.-G. Cramer, Wolfgang Paul, Ewald Niehuis, "Novel Cluster Ion Beams For Secondary Ion Generation, Sputtering And FIB/SIMS Application", Microscopy and Microanalysis 18(S2) (2012) 904-905; DOI: 10.1017/S143192761200637X.
[3] John S. Hammond, Gregory L. Fisher, Scott R. Bryan, Rait Kanarbik and Pritt Möller "FIB-TOF Tomography of Solid Oxide Fuel Cells", Microscopy and Microanalysis 19 (suppl 2) (2013) 672-673, DOI:10.1017/S1431927613005357.
[4] Quentin P. Vanbellingen, Nicolas Elie, Michael J. Eller, Serge Della-Negra, David Touboul, Alain Brunelle, "Time-of-flight secondary ion mass spectrometry imaging of biological samples with delayed extraction for high mass and high spatial resolutions" Rapid Commun. Mass Spectrom. 29 (2015) 1187–1195, DOI: 10.1002/rcm.7210

Researcher poster